Dormant origins and fork protection mechanisms rescue sister forks arrested by transcription

Alessandra Brambati[1], Luca Zardoni[1,2], Yathish Jagadheesh Achar[3], Daniele Piccini[3], Lorenzo Galanti[1], Arianna Colosio[1], Marco Foiani[3,4] and Giordano Liberi[1,3,*]

[1]Istituto di Genetica Molecolare, CNR, Via Abbiategrasso 207, 27100 Pavia, Italy, [2]Scuola Universitaria Superiore IUSS, 27100 Pavia, Italy, [3]IFOM Foundation, Via Adamello 16, 20139 Milan, Italy and [4]Università degli Studi di Milano, 20133 Milan, Italy

ABSTRACT

The yeast RNA/DNA helicase Sen1, Senataxin in human, preserves the integrity of replication forks encountering transcription by removing RNA-DNA hybrids. Here we show that, in *sen1* mutants, when a replication fork clashes head-on with transcription is arrested and, as a consequence, the progression of the sister fork moving in the opposite direction within the same replicon is also impaired. Therefore, sister forks remain coupled when one of the two forks is arrested by transcription, a fate different from that experienced by forks encountering Double Strand Breaks. We also show that dormant origins of replication are activated to ensure DNA synthesis in the proximity to the forks arrested by transcription. Dormant origin firing is not inhibited by the replication checkpoint, rather dormant origins are fired if they cannot be timely inactivated by passive replication. In *sen1* mutants, the Mre11 and Mrc1–Ctf4 complexes protect the forks arrested by transcription from processing mediated by the Exo1 nuclease. Thus, a harmless head-on replication-transcription clash resolution requires the fine-tuning of origin firing and coordination among Sen1, Exo1, Mre11 and Mrc1–Ctf4 complexes.

INTRODUCTION

Perturbations of DNA synthesis lead to replication stress, a pathologic condition that fuels genome instability in several human diseases, including cancer (1). The activation of oncogenes promotes replication stress (2,3) that has been proposed to account for the formation of precancerous DNA lesions in early tumorigenesis (1). Impaired replication fork progression and unscheduled replication origin ac-

tivation are both features of oncogene-induced replication stress (4).

Several lines of evidence suggest that transcription can affect fork progression and stability, thus contributing to replication stress (5). In human cells, increased replication-transcription conflicts have been observed upon Cyclin E or RAS overexpression, providing a link between deregulated transcription and oncogene-induced replication stress (6,7). Moreover, transcription contributes to the expression of both 'Common Fragile Sites' (CFSs) and 'Early Replicating Fragile Sites' (ERFSs), specific genomic regions prone to rearrangements under oncogene-induced replication stress (8,9). Genome alterations at transcribed genes have been also connected to perturbed replication in neural stem and progenitor cells, suggesting that transcription-replication interference could also impact on neurogenesis and neural functions (10). The unscheduled accumulation of single strand (ss) DNA and RNA-DNA hybrids to form structures called R-loops is tightly connected to the problem of transcription-induced replication stress and recombination (11). Key players in DNA damage response, including the breast cancer proteins BRCA1 and BRCA2 (12–14), the Fanconi Anemia proteins (15,16), Nucleotide Excision Repair endonucleases (17) and the RNA/DNA helicase Senataxin (18,19), have been involved in limiting R-loop accumulation and transcription-associated DNA damage. Senataxin cooperates with BRCA1 to prevent R-loop-associated DNA damage (12) and its coding gene SETX is itself a potential tumor suppressor (13,20). Moreover, SETX is mutated in the juvenile-onset neurological disorders Ataxia with Oculomotor Apraxia type 2 and Amyotrophic Lateral Sclerosis type 4 (21,22). Sen1, the yeast ortholog of Senataxin, counteracts the formation of transcription-associated recombinogenic R-loops (23) acting at the fork in head-on encounters with highly transcribed RNA Polymerase II (RNAPII) genes (24). Head-on collisions between replication and transcription are more

detrimental to fork integrity than the codirectional ones (25). Recent evidence supports the notion that a key difference in the two types of collisions is that head-on encounters stimulate R-loop accumulation (26,27).

Fork impairment triggers a checkpoint response that, in turn, promotes fork integrity maintenance and it is thought to represent the first line of defense against tumorigenesis (1). Furthermore, in the case of fork failure, nearby dormant origins can be activated to resume DNA replication. Dormant origins are normally silent and serve as backups under replication stress condition (28–32). While dormant origins are locally activated in response to DNA damage, the replication checkpoint inhibits new origin firing to prevent the generation of further damaged forks (33,34). The mechanism that regulates dormant origin firing is not entirely understood (35).

A single replication origin generates two divergent sister forks that move with comparable speed (29). However, asymmetric sister fork progression can be observed under replication stress conditions (3,16,30), suggesting that when a fork is impaired by DNA damage, the sister fork can proceed in the opposite direction within the same replicon.

Here we studied replicon dynamic in response to head-on replication-transcription collisions occurring in the absence of the RNA/DNA helicase Sen1. We found that a replication fork clashing with transcription is arrested and, as a consequence, the progression of the sister fork is also impaired. Forks impeded by transcription cannot inactivate nearby dormant origins by passive replication. Dormant origins are then fired and rescue replication in proximity to the stalled forks. Forks clashing with transcription in *sen1* mutants are stabilized by the Mre11-Rad50-Xrs2 (MRX) complex (MRN in human) and the Mrc1-Tof1-Csm3-Ctf4 complex (Claspin-Tim1-Tipin-And1 in human), which protect arrested forks from resection mediated by Exo1 nuclease.

MATERIALS AND METHODS

Yeast strains and growth conditions

All the yeast strains used in this study are isogenic derivatives of *W303–1A RAD5* and are listed in Supplementary Table S1. Deletion strains were obtained by one-step polymerase chain reaction (PCR)-targeting method. The promoter of *PDC1* gene, the *ARS consensus sequence* (ACS) of *ARS1211.5* or *ARS1211* (www.cerevisiae.oridb.org) were disrupted by Delitto Perfetto approach (36). The ACS of *ARS1210* was disrupted by one-step PCR. The conditional *sen1* mutant strain *pGAL1-URL-3HA-SEN1* has been previously described (24). An identical strategy has been employed to create the conditional *exo1* mutant strain *pGAL1-URL-3HA-EXO1* used in combination with *mre11* mutants in Figure 6. In all the experiments, yeast strains containing the *pGAL1-URL-3HA-SEN1* system and *pGAL1-URL-3HA-EXO1* and relative controls were grown in YPG (galactose at 2% w/v) and during α-factor treatment transferred to YPD (glucose at 2% w/v) to switch off Sen1 and Exo1. In these conditions Sen1 or Exo1 proteins were depleted in 30 min after galactose removal (24) (and data not shown). α-factor and HU were used to a final concentration of 2 μg/ml and 0.2M, respectively.

2D gel analysis of replication intermediates

Purification of DNA intermediates and 2D gel electrophoresis analysis were carried out as previously described (37). Briefly, samples of cells were harvested in the presence of 1% sodium azide and subjected to *in vivo* psoralen cross-linking. Replication intermediates were purified in the presence of CTAB. A total of 10 μg of DNA was digested with appropriated restriction enzymes and separated in the first dimension at 50 V for 20 h. Electrophoresis in the second dimension was carried out at 180 V for 8 h. Gels were denatured by NaOH treatment, transferred overnight onto nylon membranes in 10× Saline-Sodium Citrate (SSC) buffer and subjected to hybridization using the appropriate probes to examine replication intermediates at the genomic regions indicated in the figures. Nylon membranes were exposed on GE Healthcare Exposure cassette and images were scanned using GE Thypoon Trio™. 2D gel signals in Supplementary Figure S3B were quantified using ImageQuant 5.2 software (molecular dynamics). The levels of paused forks were calculated as the percentage of the signal relatively to that of the monomer spot and expressed as arbitrary units. Background correction was applied using the 'Object Average' mode.

BrdU-IP-chip and BrdU-IP-qPCR

The BrdU-IP chip analysis was carried out as previously described (24). Briefly, purified DNA was sheared to 500 bp by sonication, denatured and mixed with anti-BrdU monoclonal antibody (MBL M1–11-3). Antibody-bound fractions (IP) and INPUT fractions were subsequently purified and amplified by whole genome amplification kit (Sigma-Aldrich WGA1–50RXN). A total of 5 μg of amplified DNA was digested with DNaseI to a mean size of 100 bp. DNA was then purified and the fragments were end-labeled with biotin-N6-ddATP23. Hybridization, washing, staining and scanning were performed according to the manufacturer's instruction (Affymetrix).

For BrdU-IP-qPCR experiment, BrdU was added to final concentration of 200 μg/ml. DNA was extracted with Qiagen genomic DNA isolation kit, sheared to 500 bp by sonication and then denatured. A total of 10 μg of DNA were mixed overnight at 4°C with 2 μg of anti-BrdU monoclonal antibody bound to magnetic protein G beads (Invitrogen). For each sample 1 μl was taken as INPUT (2%). Input and immunoprecipitated samples were treated with protease K and RNase A before being isolated with the QIAamp DNA Mini Kit (Qiagen) and then subjected to qPCR using the SYBR Green technique (SYBR Green PCR Master Mix, Applied Biosystems). Samples were run in Roche Light Cycler 480 Real-Time PCR System. The DNA primers are listed in Supplemental Table S2. Incorporation of BrdU was determined as follows:

100×2(CT adjusted INPUT – CT IP BrdU). CT values indicate the cycle at which the exponential amplified product passes a threshold. Each reaction was performed in triplicate. The standard deviations were calculated on the basis of at least three independent experiments.

qPCR

PDC1 expression levels were measured by quantitative real-time PCR. The RNA was extracted using Qiagen RNeasy Kit. One microgram of RNA was retro-transcribed with INVILO kit (Invitrogen). qRT-PCR was done in 20 µl reaction with gene specific primers using 1 µl of cDNA diluted 1:20 using the SYBR Green Master Mix, Applied Biosystems, and run in Roche Light Cycler 480 Real-Time PCR System. qRT-PCR was also performed for *ACT1* gene from each cDNA sample.

PDC1 expression level was calculated as follows: $2^{-(CT\ test - CT\ control)}$, where test refers to the *PDC1* gene and control refers to *ACT1*. All samples were run in triplicate for each independent experiment. The standard deviations were calculated on the basis of three independent experiments.

DRIP experiments

RNA-DNA hybrids immuneprecipitation was performed as previously described (24). Briefly, purified genomic material (QIAGEN Genomic DNA kit), corresponding to 9 µg of the DNA fraction, was precipitated with sodium acetate and absolute ethanol and re-suspended in 50 µl of bidistilled water. For each sample 1 µl was taken as INPUT (2%). Then 400 µl of FA1 buffer was added (0.1% sodium dodecyl sulphate (SDS), 1% Triton X-100, 10 mM HEPES pH 7.5, 0.1% sodium deoxycholate, 275 mM NaCl). RNA-DNA hybrids were precipitated with 7.5 µg of S9.6 antibody bound to magnetic protein G beads (Invitrogen) for 90 min at 4°C. Beads were washed as previously described. Input and immunoprecipitate samples were treated with protease K and RNase A before DNA isolation with the QI-Aamp DNA Mini Kit (Qiagen), then subjected to qPCR using the SYBR Green technique (SYBR Green PCR Master Mix, Applied Biosystems) and run in Roche Light Cycler 480 Real-Time PCR System. The DNA primers were the same used to test *PDC1* levels. In Figure 4B, genomic material was incubated overnight at 37°C with or without RNase H (New England Biolabs) and then immunoprecipitated using S9.6 antibody.

Enrichment of RNA-DNA hybrids was determined as follows: 100 × 2(CT adjusted INPUT – CT IP S.6). Each reaction was performed in triplicate. The standard deviations are calculated on the basis of at least three independent experiments.

Genetic methods and other techniques

Genetic analyses were performed using standard procedures for mating, diploid selection, sporulation and tetrad dissection. For western blot analysis, protein extracts were prepared by TCA precipitation;. SDS/polyacrylamide gel electrophoresis and western blotting were performed using anti-Rad53 EL7 antibodies as previously described (24).

RESULTS

Head-on replication-transcription collisions in Sen1-depleted cells impair sister forks progression and trigger local dormant origin firing

We investigated the dynamic of replication forks colliding with transcription in the absence of Sen1. We have previously shown that Sen1 counteracts the accumulation of RNA-DNA hybrids that are formed when forks collide head-on with highly transcribed RNAPII genes (24). Here we focused our analysis on a genomic *locus* containing the highly expressed metabolic gene *PDC1*, which is closely located to the early origin of replication *ARS1211* (Figure 1A). Another feature associated with the *PDC1 locus* is the presence of the two dormant origins *ARS1211.5* and *ARS1210*, which are situated, respectively, 12.1 Kb on the right and 8.3 Kb on the left of *ARS1211* (Figure 1A). Other active origins closest to *ARS1211* are located at 75 Kb on the left and 57 Kb on the right, an inter-origin distance that is above the average in budding yeast (38). Thus, the presence of those dormant origins could be crucial in this DNA region where a high interference between replication and transcription may cause fork impairment.

Using the 2D gel method (39), we monitored the *ARS1211* right forks approaching head-on the *PDC1* gene and the replication *status* of both right and left dormant origins. Wild-type (WT) strain and cells depleted for Sen1 by means of carbon source-dependent conditional system (24) (hereafter indicated as *sen1* mutants) were released from G1 into S-phase of the cell cycle in the presence of 0.2M hydroxyurea (HU). HU-treatment triggers the Mec1-Rad53-dependent checkpoint (40) and facilitates 2D gel analysis of replication intermediates by slowing down fork progression. Consistent with our previous findings, *sen1* mutants showed a peculiar 2D gel profile when replication intermediates were analyzed at the *ARS1211-PDC1 locus* (Figure 1A) (24). These replication intermediates are sensitive to ssDNA nucleases treatment and correlate with the accumulation of both S-phase specific RNA-DNA hybrids and ssDNA-RPA nucleofilaments (24). Hence, these 2D gel structures represent replication forks paused by RNA-DNA hybrids and/or R-loops. Moreover, *sen1* mutants, but not WT cells, fired both right and left dormant origins, as indicated by the appearance of bubble-shaped intermediates (Figure 1A).

We asked whether the activation of both dormant origins in *sen1* mutants was caused by the sole replication-transcription conflict at the *PDC1* gene. We indeed found that a mutation in the promoter of the *PDC1* gene, which prevents its transcription, abolished the accumulation of paused intermediates at the *ARS1211-PDC1 locus* and the firing of both left and right dormant origins in *sen1* mutants (Figure 1A and Supplementary Figure S1A). Other dormant/late origins on Chromosome XII surrounding the region of replication-transcription conflict were not activated in *sen1* mutant, as indicated by BrdU-IP-chip genome-wide analysis (Figure 1B). Conversely, as previously shown, checkpoint-deficient *rad53* kinase mutants triggered the firing of dormant and late origins at a genome-wide level (33,34,41) (Figure 1B). We noted that Rad53 was
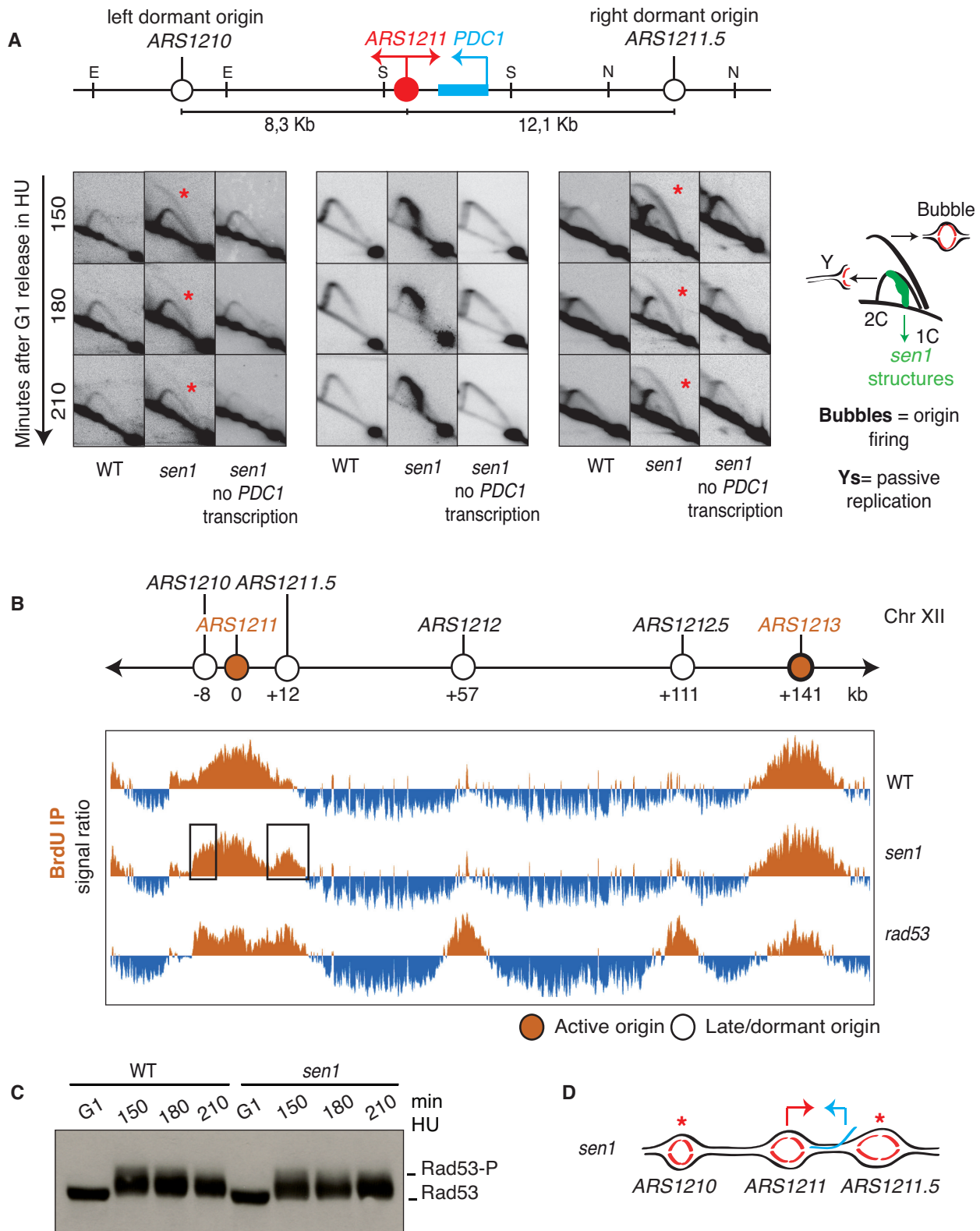
Figure 1. Head-on replication-transcription collisions trigger local dormant origin firing in *sen1* mutants. (**A**) WT (GF8), *sen1* (GF455) and *sen1* carrying a deletion of the *PDC1* promoter (GH612, *sen1 no PDC1 transcription*) were synchronized in G1 and released into 0.2M HU. Genomic DNA was digested with EcoRI (E), SphI (S) or NdeI (N) to monitor replication intermediates by 2D gel analysis at *ARS1210, ARS1211-PDC1* or *ARS1211.5 locus*, respectively. Asterisks indicate replication initiation events. A schematic representation of 2D gel replication intermediates and *sen1* specific structures (in green) is shown on the right. (**B**) BrdU-IP-chip analysis was carried out on WT (GH132), *sen1* (GH344) and *rad53K227A* (GH100) cells treated with 0.2M HU for 90 min. Orange peaks indicate active origins on a representative region of Chromosome XII containing the *ARS1211-PDC1 locus*. Position of replication origins is also shown at the top. (**C**) Rad53 phosphorylation was monitored by western blotting in WT and *sen1* strains treated as in panel A. (**D**) Schematic representation of replicon dynamic in *sen1* mutants.

active at similar levels in both WT and *sen1* HU-treated cells (Figure 1C). Moreover, in *sen1* mutants, dormant origins were activated also in unperturbed conditions, that is, when fork speed was reduced by lowering the temperature to 16°C instead of using the replication inhibitor HU (Supplementary Figure S1B).

We conclude that, in *sen1* mutants, head-on clashes between the *ARS1211* rightward moving forks and *PDC1* transcription trigger the activation of the most proximal dormant origins placed on the opposite sides of the conflict region (Figure 1D). Dormant origin firing in *sen1* mutants is a local event, it occurs despite Rad53 checkpoint activation and it is not influenced by HU-treatment.

It is possible that forks arising from the dormant origin *ARS1211.5* and moving leftward toward the region of replication-transcription conflict may contribute to rescue the replication of the *PDC1 locus*, especially if the right forks originating from the early origin undergo an irreversible arrest. To test this hypothesis, the *ACS* element of *ARS1211.5* was deleted to prevent right dormant origin activation. Formation of the *sen1* structures and fork progression at the *ARS1211* region were then monitored by 2D gel analysis. WT cells, *sen1* mutants and *sen1* mutants carrying the inactive right dormant origin (*sen1 ARS1211.5Δ*) were released from G1 into HU. In WT and *sen1* strains, the early origin *ARS1211* was activated within 30 min from G1-release, as indicated by the formation of the bubble-shaped intermediates (Figure 2A). Paused forks were detected at the *PDC1 locus* in both *sen1* and *sen1* mutated for the right dormant origin (Figure 2A and Supplementary Figure S2A). Therefore, the accumulation of the *sen1* paused forks is not influenced by forks approaching from the right dormant origin, while it depends on *PDC1* transcription (Figure 1A). In *sen1* mutants the right dormant origin was fired at ∼90 min after G1 release, following the accumulation of the 2D gels structures at the *PDC1* gene (Figure 2A). Y-shaped intermediates are observed at the *ARS1211.5 locus* before origin firing. Given that *ARS1211* is the closest active origin in the proximity of this *locus* (Figure 1A), one possibility is that a fraction of forks coming from the early origin is able to bypass the transcription block imposed by *PDC1* expression and passively replicates *ARS1211.5* (Figure 2A). Furthermore, differently from WT cells, in *sen1 ARS1211.5Δ* mutants, the relative levels of replication intermediates at the *ARS1211.5 locus* did not increase with time (Figure 2A). This suggests that the majority of the *ARS1211* forks approaching head-on *PDC1* transcription failed to proceed across adjacent regions. We conclude that, once the early origin *ARS1211* has been activated, the majority of the forks encountering head-on *PDC1* transcription are arrested in the absence of Sen1. Then, the unresolved replication-transcription conflict at *PDC1* triggers the firing of the nearest dormant origin on the right to rescue the blocked forks.

The finding that the left dormant origin *ARS1210* was also fired in *sen1* mutants in response to *PDC1* transcription (Figure 1A), raises the possibility that the progression of the *ARS1211* leftward moving fork was also prevented by the replication-transcription conflict occurring at the *PDC1* gene. To test this hypothesis, we inactivated the *ARS1210* origin in WT and *sen1* strains and we then monitored the

progression of the *ARS1211* forks by BrdU-IP followed by qPCR analysis. Noteworthy, in an *ARS1210Δ* strain, the closest active origin to *ARS1211* on the left, *ARS1209*, is 75 kb away. This gave us the opportunity to follow in a large time window the progression of the sole *ARS1211* leftward moving forks before the arrival of *ARS1209* forks from the opposite direction. WT and *sen1* strains both carrying the deleted dormant origin *ARS1210* were released from G1 into unperturbed S-phase at 16°C. At the time points indicated in Figure 2B, DNA samples were subjected to BrdU-IP-qPCR analysis to monitor nascent DNA strands at the *ARS1211 locus*. BrdU was immunoprecipitated at similar levels across *ARS1211* in WT and *sen1* mutants at 60–90 min from G1 release indicating that this origin is activated at the same time in the two strains in agreement with 2D gel analysis results. At later time points, in *sen1* mutants, we found less BrdU incorporation in this region reflecting that forks had been arrested by *PDC1* transcription. In all the other DNA regions flanking the origin, we monitored reduced levels of BrdU incorporation in *sen1* mutants compared to WT, with a greater difference in the region downstream of the *PDC1* gene. These results indicate that, in *sen1* mutants under unperturbed conditions, not only the *ARS1211* rightward moving fork is arrested at the *PDC1* gene, but also the progression of the sister fork is slowed down.

We then decided to investigate the mechanism responsible for the activation of dormant origins in *sen1* mutants in response to replication-transcription collisions at the *PDC1* gene. It is possible that both the left and right dormant origins are fired in *sen1* mutants because they cannot be passively replicated and thus inactivated by the adjacent *ARS1211* early replicating forks. Alternatively, the accumulation of arrested forks at the *PDC1* gene may generate a 'local signal' for dormant origin firing. To distinguish between these two models, we inactivated the early origin *ARS1211* and monitored, in HU-treated cells, the firing of nearby dormant origins by 2D gel analysis. As shown in Figure 3, bubble arc signals were observed at either left or right dormant origins in the *ARS1211Δ* strain but not in WT cells. Despite the fact that stalled forks did not accumulate at the *PDC1 locus* and the checkpoint was activated by HU-treatment, the firing of dormant origins was still triggered. Therefore, our data indicate that dormant origins are fired because they cannot be timely inactivated by *ARS1211* fork passage. Notably, since in *sen1* mutants the *PDC1* transcription causes the activation of both left and right dormant origins, the *PDC1* transcription must be the cause of the delayed arrival of both *ARS1211* sister forks (Figure 1A). This indicates that *PDC1* transcription not only impairs the progression of the fork that it encounters head-on, but it also prevents the progression of the sister fork moving in the opposite direction within the same replicon.

Mre11-dependent complex and Mrc1/Tof1/Ctf4 components of the replication progression complex protect transcription-arrested forks from Exo1-dependent processing

We found that, in *sen1* mutants, arrested forks at the *PDC1* gene were stable even after a prolonged HU-treatment (Sup-
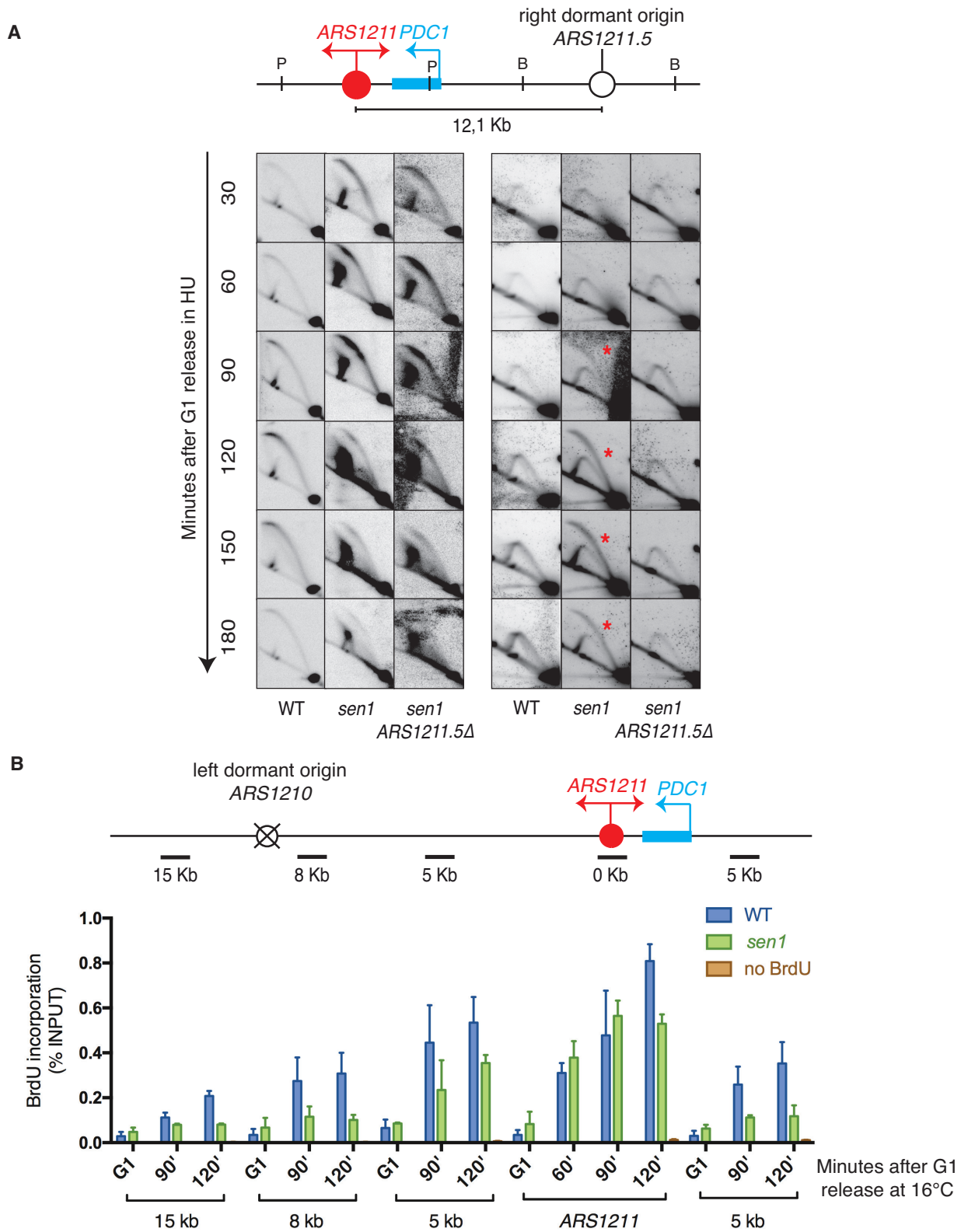
Figure 2. Replication forks are arrested upon clashing with *PDC1* transcription in *sen1* mutants. (**A**) WT, *sen1* and *sen1* mutants carrying mutated right dormant origin (GH551, *sen1 ARS1211.5Δ*) were synchronized in G1 and released into 0.2M HU. Genomic DNA was digested with PvuII (P) or with BclI (B) to monitor replication intermediates by 2D gel analysis, respectively, at *ARS1211-PDC1* or *ARS1211.5 locus.* Asterisks indicate replication initiation events. (**B**) WT and *sen1* mutants carrying deleted *ARS1210* dormant origin (GH977 and GH979) were synchronized in G1 and released into the cell cycle at 16°C in the presence of BrdU. BrdU incorporation was monitored at the indicated DNA regions by BrdU-IP qPCR. Data are represented as mean ± SD on the basis of three independent experiments.
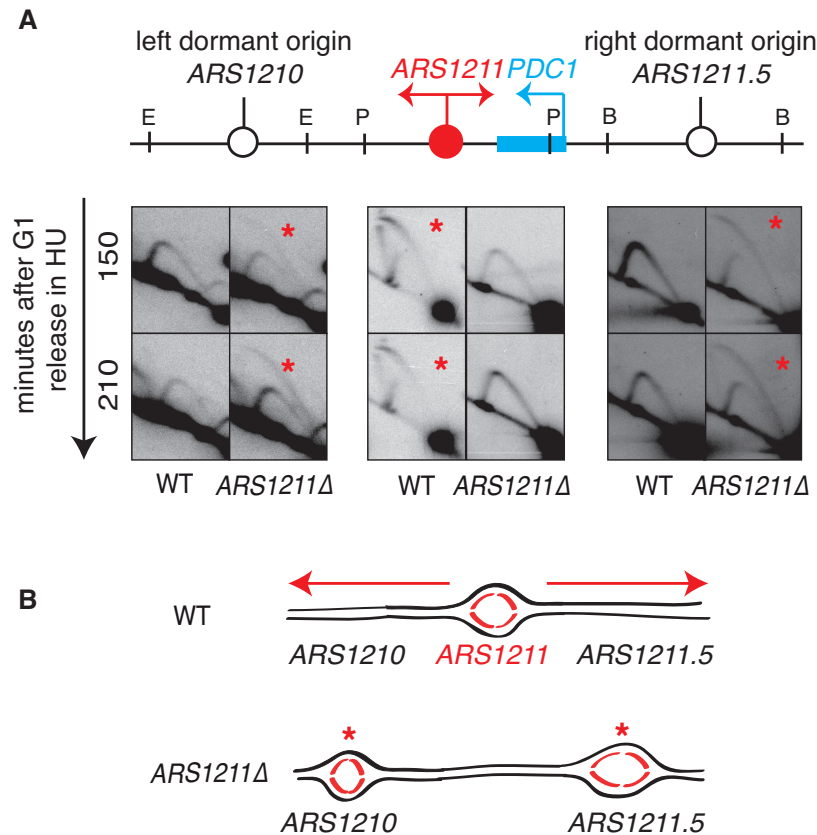
Figure 3. Inactivation of the early origin *ARS1211* triggers the firing of the right and left dormant origins. (**A**) WT and cells carrying the mutated early origin *ARS1211* (GH876, *ARS1211Δ*) were synchronized in G1 and released into 0.2M HU. Genomic DNA was digested with EcoRI (E), PvuII (P) or BclI (B) to monitor replication intermediates by 2D gel analysis, respectively, at *ARS1210, ARS1211-PDC1* or *ARS1211.5 locus*. Asterisks indicate replication initiation events. (**B**) Schematic representation of replication origins activation in WT and *ARS1211Δ* mutants.

plementary Figure S2B), suggesting that specific pathways may stabilize forks arrested by transcription and/or counteract abnormal fork transitions in S-phase. The MRX complex and Mrc1–Tof1–Ctf4 components of the replication progression complex (RPC) are required for *sen1–1* hypomorphic mutant viability (23,24). Hence, we thought that those protein complexes could be ideal candidates for a role in stabilizing transcription-arrested forks. Deletions in the genes encoding Mre11 or Mrc1–Tof1–Ctf4 complexes were combined with the conditional *sen1* strain and the double mutants were analyzed by 2D gel technique to monitor transcription-dependent replication intermediates at *ARS1211-PDC1 locus* in HU. We found that the inactivation of the MRX complex or RPC did not impair replication at *PDC1* gene, while it partially prevented the accumulation of both paused forks and S-phase specific RNA-DNA hybrids in *sen1* mutants (Figure 4; Supplementary Figure S3A and B). Previous studies have shown that Mre11 and Mrc1 associate with replication forks, although they are not needed for origin firing (41–43). Conversely, HU-treated *mrc1* mutants display increased number of fired origins due to their checkpoint defects (41). We found that in *sen1 mre11* or *sen1 mrc1* double mutants the firing of *ARS1211* origin was not affected when *PDC1* transcription was prevented (Supplementary Figure S3C). Moreover, neither *mre11* nor *mrc1* mutations affected *PDC1* expression (Supplementary

Figure S3D). This suggests that the decreased accumulation of arrested forks in *sen1 mre11* or *sen1 mrc1* double mutants cannot be ascribed to a reduced replication-transcription conflict at the *PDC1* gene. Hence, we conclude that the Mre11- and Mrc1-dependent complexes are required for the accumulation of both stalled forks and RNA-DNA hybrids at the *PDC1 locus* in *sen1* mutants.

Both MRX and RPC play multiple roles in the DNA damage response (44). MRX is required for nuclease-mediated Double Strand Break (DSB) ends processing in homologous recombination (HR) and Mrc1 is required to amplify the replication checkpoint signal. We found that the point mutant *mre11D56N*, which eliminates Mre11 nuclease activity without compromising MRX complex integrity (45), had no effect on the stability of *sen1* forks arrested at the *PDC1* gene and it was not lethal in combination with *sen1–1* hypomorphic mutant (Figure 4). Thus, the integrity of MRX complex, rather than its nuclease activity, is crucial to deal with the *sen1* replication problems. Mrc1, together with other RPC components, coordinates replisome activities and, in response to replication stress, is phosphorylated by Mec1 to initiate a robust Rad53-dependent checkpoint response (40). To address whether the function of Mrc1 at forks in *sen1* mutants was dependent on its role in replication or in checkpoint activation, we examined the separation of function *mrc1-AQ* allele. The defective Mrc1-AQ
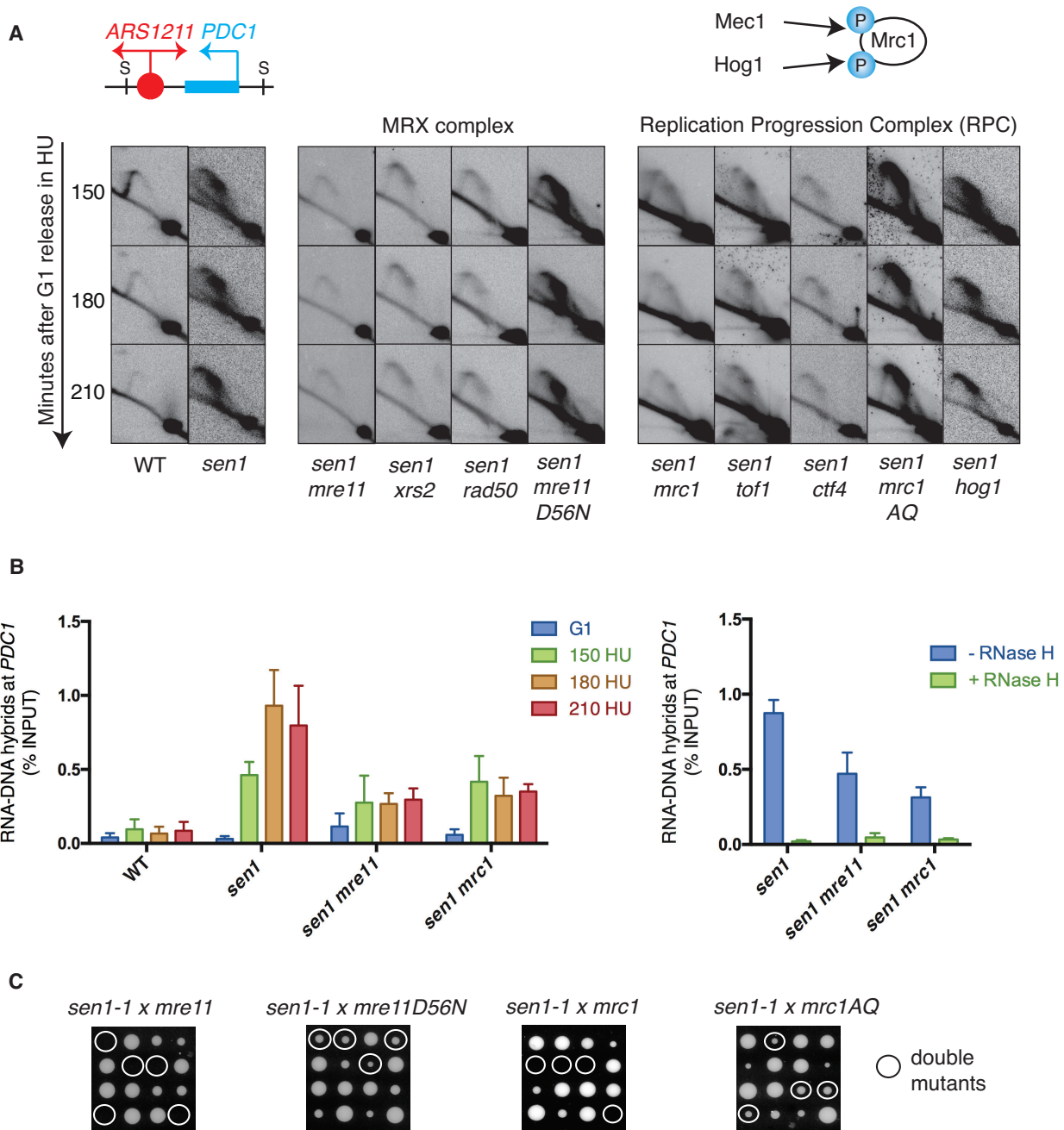
Figure 4. Accumulation of arrested forks and RNA-DNA hybrids upon unscheduled replication-transcription collisions depends on the MRX and RPC complexes. (**A**) WT *sen1*, *sen1 mre11* (GH169), *sen1 xrs2* (GH538), *sen1 rad50* (GH535), *sen1 mre11D56N* (GH531), *sen1 mrc1* (GH469), *sen1 tof1* (GH578), *sen1 ctf4* (GH472), *sen1 mrc1AQ* (GH560) and *sen1 hog1* (GH574) were synchronized in G1 and released into 0.2M HU. Genomic DNA was digested with SphI (S) to monitor replication intermediates by 2D gel analysis at *ARS1211-PDC1 locus*. Mec1 and Hog1 kinases target the Mrc1 subunit of RPC under different replication stress stimuli (cartoon on the top). (**B**) RNA-DNA hybrids accumulation was analyzed by DRIP-qPCR at *PDC1* gene in WT, *sen1*, *sen1 mre11* and *sen1 mrc1* cells treated as in panel A. For each strain, genomic material of a representative time point (180 min) was treated or not with RNaseH and than subjected to DRIP-qPCR to monitor RNA-DNA hybrids accumulation at the *PDC1* gene. Data are represented as mean ± SD on the basis of four independent experiments. (**C**) Tetrads obtained from sporulation of diploids heterozygous for the indicated mutations were grown at 30°C. Double mutant spores are indicated by the white circles.

protein still binds to replication forks but it is unable to activate the checkpoint response (42). As shown in Figure 4, *sen1–1 mrc1-AQ* mutants were viable and fork arrest was still observed at the *PDC1* gene. Thus, the essential function of Mrc1 in *sen1* mutants is not linked to its role in checkpoint activation. Mrc1 is also phosphorylated by the Hog1 kinase to regulate transcription-replication conflicts caused by osmotic stress (46), even though we found that this modification was also not required for the stability of forks arrested at the *PDC1* gene in *sen1* mutants (Figure 4A).

Taken together, our data suggest a structural role for both MRX and RPC to stabilize transcription-arrested forks and to promote cell viability in *sen1* mutants.

The disappearance of *sen1* 2D gels structures when MRX or RPC are inactivated may suggest that forks escape the *PDC1*-dependent transcription block and move forward. To test this hypothesis, we monitored fork progression in WT, *sen1*, *sen1 mre11* and *sen1 mrc1* strains carrying the mutated right dormant origin. Differently from WT cells, all mutant strains exhibited barely detectable Y-shaped arcs in the chromosomal fragments downstream the *PDC1* replication-transcription collision site (Figure 5A). Therefore, *ARS1211* forks approaching the *PDC1* gene were still arrested by transcription in *sen1 mre11* or *sen1 mrc1* double mutants. While forks arising from *ARS1211* could not bypass *PDC1* transcription in *sen1*, *sen1 mre11* or *sen1 mrc1* mutants, forks coming in the opposite direction from right dormant origin could approach the *PDC1 locus* (Figure 5B). Thus, Mrc1 and Mre11 are required to stabilize the forks arrested by head-on collisions with *PDC1* transcription in *sen1* mutants. Based on these results, we hypothesized that, in *sen1 mrc1* or *sen1 mre11* mutants, stalled forks could be prematurely processed in S-phase by specific nuclease-dependent pathways. Supporting this idea, we found that the inactivation of Exo1 nuclease in *sen1 mrc1* or *sen1 mre11* mutants restored a *sen1*-like 2D gel profile with partial accumulation of the arrested forks at the *PDC1* gene (Figure 6). Exo1 inactivation did not interfere with the accumulation of transcription-dependent structures at the *PDC1 locus* in *sen1* single mutants (data not shown). Moreover, inactivation of *RAD51*, a central player in the HR-dependent pathway, had no effect on the dynamic of *sen1* structures accumulation in *mrc1* mutants (Figure 6).

Taken together these results indicate that, through an HR-independent mechanism, Exo1 nuclease resects *sen1* forks arrested by transcription in the absence of MRX or RPC.

DISCUSSION

Uncoordinated replication-transcription collisions, leading to pathological R-loop accumulation, are a major source of intrinsic replication stress and genome instability, which are hallmarks of cancer and other human diseases (5). Cells have evolved different strategies to coordinate replication with transcription and to remove RNA-DNA hybrids/R-loops, one of which depends on the activity of the Senataxin/Sen1 RNA/DNA helicase. Sen1 acts at head-on replication-transcription collisions (24), a type of clashes particularly dangerous for genome integrity maintenance (5).
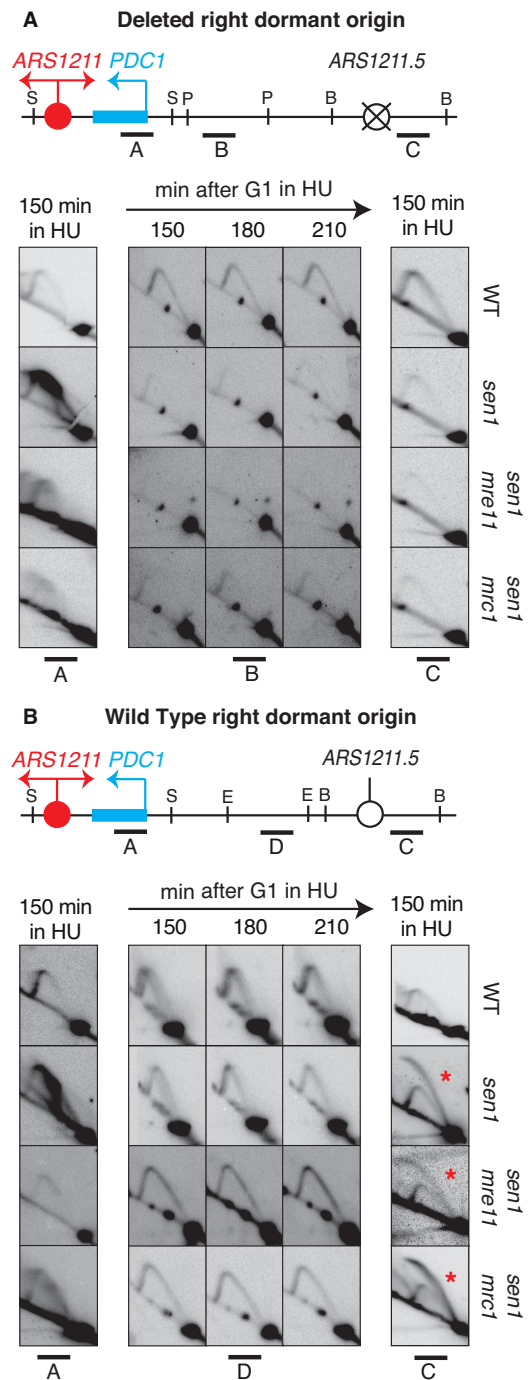

Figure 5. Fork progression analysis across *PDC1* transcription. (**A**) WT (GH551), *sen1, sen1 mre11* (GH566) and *sen1 mrc1* cells (GH586) carrying the mutated right dormant origin (*ARS1211.5Δ*) were synchronized in G1 and released into 0.2M HU. Genomic DNA was digested with PstI and hybridized with probe B to monitor replication intermediates at the indicated time points by 2D gel analysis in a fragment downstream the *PDC1* gene. 2D gel analysis of intermediates at *ARS1211-PDC1* (probe A, SphI) and *ARS1211.5* (probe C, BclI) *loci* is also shown at one representative time point. (**B**) WT, *sen1, sen1 mre11* and *sen1 mrc1* cells (non-mutated for *ARS1211.5*) were treated as in panel A. Genomic DNA was digested with EcoRI and hybridized with probe D to monitor replication intermediates at the indicated time points by 2D gel analysis in a fragment downstream the *PDC1* gene. 2D gel analysis of intermediates at *ARS1211-PDC1* (probe A, SphI) and *ARS1211.5* (probe C, BclI) *loci* is also shown at one representative time point.
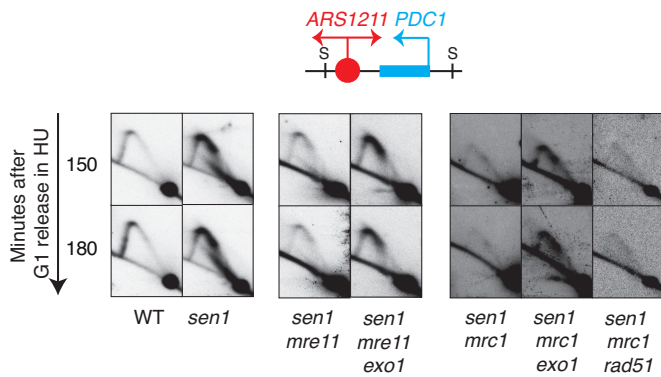
Figure 6. MRX and RPC complexes protect *sen1* forks arrested by transcription from Exo1-dependent resection. WT, *sen1*, *sen1 mre11*, *sen1 mre11 exo1* (GH869), *sen1 mrc1*, *sen1 mrc1 exo1* (GH790) and *sen1 mrc1 rad51* (GH718) were synchronized in G1 and released into 0.2M HU. Genomic DNA was digested with SphI (S) to monitor replication intermediates by 2D gels at *ARS1211-PDC1 locus*.

In this study, we characterized the fork dynamic at an early replicating and highly transcribed domain in budding yeast that resembles a new class of human fragile sites called ERFSs ([8]). We focused our study on a natural DNA region that includes the highly expressed *PDC1* metabolic gene, whose transcription encounters head-on the forks originating from the early origin *ARS1211*. The *ARS1211-PDC1 locus* is flanked by two dormant origins, whose presence reduces the inter-origin gap in a region that, not only is poor of other active origins, but is also at high risk for fork stalling due to transcription. Such feature allows us also to investigate the impact of head-on replication-transcription collisions on dormant origin firing.

We found that, in *sen1* mutants, the replication fork encountering head-on *PDC1* transcription is arrested and this impairs the progression of the sister fork in the same replicon. Forks arrested by transcription in *sen1* mutants are rescued by two mechanisms: the first relays on the local activation of nearby dormant origins and the second on the joint activities of Mre11- and Mrc1/Ctf4-dependent complexes that counteract the Exo1-mediated processing of arrested forks (Figure [7]).

In particular, the forks arising from the right dormant origin encounter *PDC1* transcription codirectionally, that is, in a less dangerous type of clash (Figure [7]). In this way, R-loops could be resolved at the topological level ([5]) or by the replisome-associated helicase ([26]) and in any case without the need for a specialized RNA/DNA helicase. It remains to be investigated whether highly transcribed genes are frequently located nearby dormant origins as in the case of the *PDC1* gene. We note that other sites of head-on replication-transcription conflicts that require Sen1 helicase for their resolution are located in the proximity to other efficient origins ([24]). The scheduled activation of these origins can rescue the forks arrested by transcription without the need for new origin firing. This could be a most common strategy to complete replication in response to transcription interference in budding yeast, which has a compact genome with many efficient origins of replication. A defense mecha-

nism based on dormant origin activation against the deleterious consequences of replication-transcription clashes and R-loop accumulation could be crucial in mammals. Recent evidence indicates that inhibition of origin firing enhances the formation of R-loops, which preferentially accumulate in head-on replication-transcription collisions ([26]). R-loop accumulation, increased transcription-replication interference and new origin firing are all signatures of endogenous replication stress ([3,6,7]) and the failure to activate dormant origins in response to endogenous replication stress increases DNA damage and cancer risk ([47]).

Other reports have shown that dormant origins are locally activated in response to fork failure ([28–32]) and the replication checkpoint represses new origin firing ([33,34]). Whether this is an active mechanism promoted by impaired forks remains unclear ([28,30]). Here we showed that the local firing of dormant origins is induced when the progression of *ARS1211* early replicating forks is prevented by transcription in checkpoint-activated *sen1* mutants. Moreover, dormant origins are also fired when replication forks never start at *ARS1211* in checkpoint-activated WT cells. Thus, dormant origin firing is not inhibited by the checkpoint and it is not triggered by the accumulation of stalled forks. Our results are consistent with the prediction that dormant origins behave like fully competent late origins, which never have the opportunity to fire unless their passive replication is prevented ([28,48]).

We found that the left and right dormant origins are both activated in response to unscheduled replication-transcription collisions at the *PDC1* gene and both the *ARS1211* sister forks are slowed down in *sen1* mutants. Hence, we concluded that the conflict at the *PDC1 locus* interferes with the progression of both *ARS1211* sister forks. Thus, when one fork is arrested by *PDC1* transcription, the sister fork moving in the opposite direction is also impaired reflecting some degree of coupling of sister replisomes activities (Figure [7]). Since the *PDC1* gene is located 1Kb away from *ARS1211*, fork progression is aborted very early by transcription in *sen1* mutants. Although our data suggest a coordination in sister forks progression at the beginning of the DNA synthesis, they do not exclude that sister forks are also coupled at later stages. Despite these different possibilities, our findings suggest that a single head-on replication-transcription clash can disrupt bi-directional replication.

The 'double replisome' model for DNA replication suggests that the sister replisomes are associated into fixed 'replication factories', which synthesize the two halves of a replicon in a coordinated fashion ([49,50]). Conflicting evidence supporting ([51–53]) or disproving ([30,54,55]) this model has been collected. In yeast, it has been shown that when a replication fork is arrested by a DSB, the progression of the sister fork is not impeded ([30]). Our findings are not at odds with this observation, since we failed to observe DSBs accumulation by Pulsed Field Gel Electrophoresis at the *PDC1 locus* in *sen1* mutants (data not shown). It is conceivable that a DSB disrupts replicon topology, which could be instead maintained during a replication-transcription clash and could be crucial to the association of the sister replisomes (Figure [7]). Therefore, we conclude that the sister replisomes are coupled or uncoupled under different conditions of replication stress.
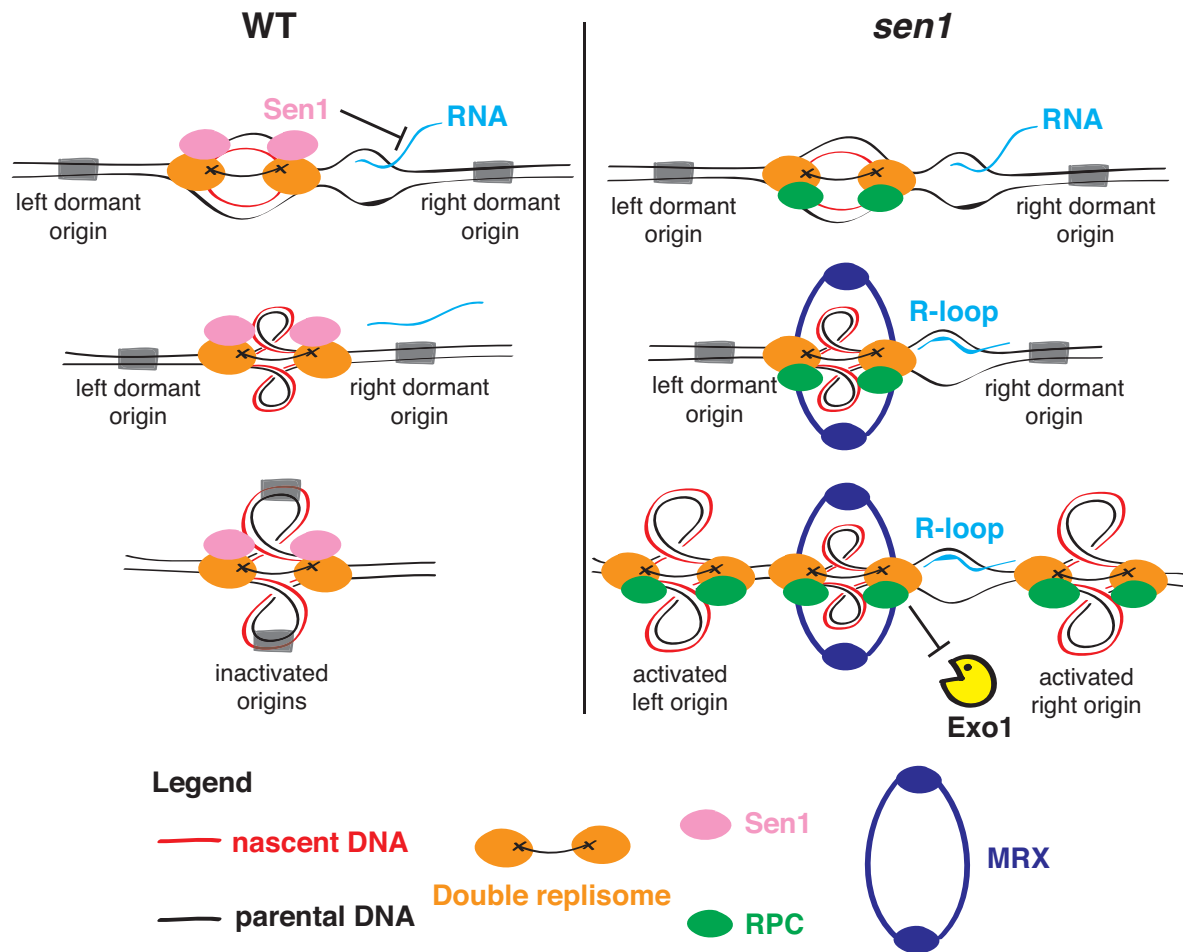
Figure 7. Mechanisms rescuing replication forks arrested by transcription. (**Left panel**) DNA is pulled into fixed double replisome during DNA synthesis and the two halves of the replicon are replicated in a coordinated manner. Sen1 RNA/DNA helicase associates with replication forks and, by displacing nascent RNA in head-on encounter with transcription, prevents the accumulation of R-loops. (**Right panel**) In *sen1* mutants, RNA-DNA hybrids/R-loops arrest the progression of both sister forks. Nearby dormant origins cannot be inactivated by passive replication and they have enough time to fire. Forks initiated by the right dormant origin rescue stalled forks with a less detrimental co-directional encounter with transcription. Fork arrested by transcription are stabilized by RPC components of the replisome and the MRX complex, which is recruited at stalled forks. RPC and MRX help to maintain the topological integrity of the replicon, prevent RNA-DNA hybrids destabilization and Exo1-mediated resection of the arrested forks. See the text for further details.

We showed that R-loops are stabilized during head-on encounters with replication forks. Thus, while R-loops contribute to arrest fork progression, they are not processed in S-phase. As mentioned above, a more timely option could be to resolve R-loops co-directionally in the absence of Sen1 using a fork coming from a nearby origin. We show that the stability of arrested forks and RNA-DNA hybrids in *sen1* mutants is enhanced by the MRX complex and the Mrc1/Tof1/Ctf4 components of RPC. These protein complexes counteract the Exo1-mediated processing of *sen1* forks arrested by transcription. The role of Exo1 at *sen1* forks in RPC or MRX mutants resembles that observed in *rad53* checkpoint-deficient mutants, where the nuclease promotes the unscheduled resection of HU-stalled forks following replisome disassembly (56). Our data do not exclude that Exo1, a member of the conserved Rad2/XPG nuclease family, processes RNA-DNA hybrids at the fork. Rad2/XPG is a structure-specific DNA nuclease that has been proposed to remove R-loops by cleavage (17), while

Exo1 could degrade RNA-DNA hybrids using its intrinsic RNaseH activity (57). Mrc1, Ctf4, Tof1 and Csm3 proteins cooperate at the replisome to physically and functionally link DNA polymerases with DNA helicase and their inactivation impairs proper fork progression and replisome stability under replication stress conditions (44). The function of these evolutionarily conserved replisome-associated factors appears crucial to promote fork progression through hard-to-replicate sites (44). Here we found that these factors are also crucial in head-on replication-transcription collisions where they could play, in cooperation with the MRX complex, a structural function in stabilizing the forks arrested by transcription (Figure 7). MRX has been involved in the processing of DSB ends and stalled forks (44). We showed that, at transcription-arrested forks, MRX rather counteracts Exo1 nucleolytic activity independently of its function in the HR pathway. Thus, MRX activity here is more consistent with a nuclease-independent structural role implicating it in the maintenance of the fork integrity, per-

haps by tethering sister chromatids together, as previously proposed (43,58,59) (Figure 7).

Overall our results provide novel mechanistic insights into how cells cope with the accumulation of dangerous R-loops during a head-on replication-transcription collision. Our findings help to explain how replication-dependent DNA lesions could accumulate in early tumorigenesis in the absence of certain crucial fork-protection factors, such as Senataxin. It has been shown that fork protection mechanisms contribute to chemotherapy drug resistance in BRCA-deficient tumor cells (60). We note that our data suggest possible strategies used by tumor cells to rescue fork-dependent defects and escape the checkpoint-dependent barrier in cancer progression. Senataxin and the MRN complex have been also implicated in neurological disorders, which include certain severe hereditary forms of Ataxia (21,22,61). Since replication-transcription collisions are potential sources of chromosomal rearrangements in neural stem/progenitor cells (10), our findings could also have implications for the development of the diseases caused by dysfunctions of Senataxin and/or the MRN complex.

AVAILABILITY

Genome-Wide Analysis of DNA Synthesis by BrdU Immunoprecipitation on Tiling Microarrays (BrdU-IP-chip) is available on GEO (accession number GSE 97046).

SUPPLEMENTARY DATA

Supplementary Data are available at NAR Online.

ACKNOWLEDGEMENTS

FUNDING

REFERENCES

1. Halazonetis,T.D., Gorgoulis,V.G. and Bartek,J. (2008) An oncogene-induced DNA damage model for cancer development. *Science*, **319**, 1352–1355.
2. Bartkova,J., Rezaei,N., Liontos,M., Karakaidos,P., Kletsas,D., Issaeva,N., Vassiliou,L.V., Kolettas,E., Niforou,K., Zoumpourlis,V.C. *et al.* (2006) Oncogene-induced senescence is part of the tumorigenesis barrier imposed by DNA damage checkpoints. *Nature*, **444**, 633–637.
3. Di Micco,R., Fumagalli,M., Cicalese,A., Piccinin,S., Gasparini,P., Luise,C., Schurra,C., Garre,M., Nuciforo,P.G., Bensimon,A. *et al.* (2006) Oncogene-induced senescence is a DNA damage response triggered by DNA hyper-replication. *Nature*, **444**, 638–642.
4. Hills,S.A. and Diffley,J.F. (2014) DNA replication and oncogene-induced replicative stress. *Curr. Biol.*, **24**, R435–R444.
5. Bermejo,R., Lai,M.S. and Foiani,M. (2012) Preventing replication stress to maintain genome stability: resolving conflicts between replication and transcription. *Mol. Cell*, **45**, 710–718.
6. Jones,R.M., Mortusewicz,O., Afzal,I., Lorvellec,M., Garcia,P., Helleday,T. and Petermann,E. (2012) Increased replication initiation and conflicts with transcription underlie Cyclin E-induced replication stress. *Oncogene*, **32**, 3744–3753.
7. Kotsantis,P., Silva,L.M., Irmscher,S., Jones,R.M., Folkes,L., Gromak,N. and Petermann,E. (2016) Increased global transcription activity as a mechanism of replication stress in cancer. *Nat. Commun.*, **7**, 13087.
8. Barlow,J.H., Faryabi,R.B., Callen,E., Wong,N., Malhowski,A., Chen,H.T., Gutierrez-Cruz,G., Sun,H.W., McKinnon,P., Wright,G. *et al.* (2013) Identification of early replicating fragile sites that contribute to genome instability. *Cell*, **152**, 620–632.
9. Helmrich,A., Ballarino,M. and Tora,L. (2011) Collisions between replication and transcription complexes cause common fragile site instability at the longest human genes. *Mol. Cell*, **44**, 966–977.
10. Wei,P.C., Chang,A.N., Kao,J., Du,Z., Meyers,R.M., Alt,F.W. and Schwer,B. (2016) Long neural genes harbor recurrent dna break clusters in neural stem/progenitor cells. *Cell*, **164**, 644–655.
11. Santos-Pereira,J.M. and Aguilera,A. (2015) R loops: new modulators of genome dynamics and function. *Nat. Rev. Genet.*, **16**, 583–597.
12. Hatchi,E., Skourti-Stathaki,K., Ventz,S., Pinello,L., Yen,A., Kamieniarz-Gdula,K., Dimitrov,S., Pathania,S., McKinney,K.M., Eaton,M.L. *et al.* (2015) BRCA1 recruitment to transcriptional pause sites is required for R-loop-driven DNA damage repair. *Mol. Cell*, **57**, 636–647.
13. Hill,S.J., Rolland,T., Adelmant,G., Xia,X., Owen,M.S., Dricot,A., Zack,T.I., Sahni,N., Jacob,Y., Hao,T. *et al.* (2014) Systematic screening reveals a role for BRCA1 in the response to transcription-associated DNA damage. *Genes Dev.*, **28**, 1957–1975.
14. Bhatia,V., Barroso,S.I., Garcia-Rubio,M.L., Tumini,E., Herrera-Moyano,E. and Aguilera,A. (2014) BRCA2 prevents R-loop accumulation and associates with TREX-2 mRNA export factor PCID2. *Nature*, **511**, 362–365.
15. Garcia-Rubio,M.L., Perez-Calero,C., Barroso,S.I., Tumini,E., Herrera-Moyano,E., Rosado,I.V. and Aguilera,A. (2015) The fanconi anemia pathway protects genome integrity from R-loops. *PLoS Genet.*, **11**, e1005674.
16. Schwab,R.A., Nieminuszczy,J., Shah,F., Langton,J., Lopez Martinez,D., Liang,C.C., Cohn,M.A., Gibbons,R.J., Deans,A.J. and Niedzwiedz,W. (2015) The Fanconi anemia pathway maintains genome stability by coordinating replication and transcription. *Mol. Cell*, **60**, 351–361.
17. Sollier,J., Stork,C.T., Garcia-Rubio,M.L., Paulsen,R.D., Aguilera,A. and Cimprich,K.A. (2014) Transcription-coupled nucleotide excision repair factors promote R-loop-induced genome instability. *Mol. Cell*, **56**, 777–785.
18. Skourti-Stathaki,K., Proudfoot,N.J. and Gromak,N. (2011) Human senataxin resolves RNA/DNA hybrids formed at transcriptional pause sites to promote Xrn2-dependent termination. *Mol. Cell*, **42**, 794–805.
19. Yuce,O. and West,S.C. (2013) Senataxin, defective in the neurodegenerative disorder ataxia with oculomotor apraxia 2, lies at the interface of transcription and the DNA damage response. *Mol. Cell. Biol.*, **33**, 406–417.
20. Zhao,Q., Kirkness,E.F., Caballero,O.L., Galante,P.A., Parmigiani,R.B., Edsall,L., Kuan,S., Ye,Z., Levy,S., Vasconcelos,A.T. *et al.* (2010) Systematic detection of putative tumor suppressor genes through the combined use of exome and transcriptome sequencing. *Genome Biol.*, **11**, R114.
21. Moreira,M.C., Klur,S., Watanabe,M., Nemeth,A.H., Le Ber,I., Moniz,J.C., Tranchant,C., Aubourg,P., Tazir,M., Schols,L. *et al.* (2004) Senataxin, the ortholog of a yeast RNA helicase, is mutant in ataxia-ocular apraxia 2. *Nat. Genet.*, **36**, 225–227.
22. Chen,Y.Z., Bennett,C.L., Huynh,H.M., Blair,I.P., Puls,I., Irobi,J., Dierick,I., Abel,A., Kennerson,M.L., Rabin,B.A. *et al.* (2004) DNA/RNA helicase gene mutations in a form of juvenile amyotrophic lateral sclerosis (ALS4). *Am. J. Hum. Genet.*, **74**, 1128–1135.

23. Mischo,H.E., Gomez-Gonzalez,B., Grzechnik,P., Rondon,A.G., Wei,W., Steinmetz,L., Aguilera,A. and Proudfoot,N.J. (2011) Yeast Sen1 helicase protects the genome from transcription-associated instability. *Mol. Cell*, **41**, 21–32.

24. Alzu,A., Bermejo,R., Begnis,M., Lucca,C., Piccini,D., Carotenuto,W., Saponaro,M., Brambati,A., Cocito,A., Foiani,M. *et al.* (2012) Senataxin associates with replication forks to protect fork integrity across RNA-polymerase-II-transcribed genes. *Cell*, **151**, 835–846.

25. Prado,F. and Aguilera,A. (2005) Impairment of replication fork progression mediates RNA polII transcription-associated recombination. *EMBO J.*, **24**, 1267–1276.

26. Hamperl,S., Bocek,M.J., Saldivar,J.C., Swigut,T. and Cimprich,K.A. (2017) Transcription-replication conflict orientation modulates R-loop levels and activates distinct DNA damage responses. *Cell*, **170**, 774–786.

27. Lang,K.S., Hall,A.N., Merrikh,C.N., Ragheb,M., Tabakh,H., Pollock,A.J., Woodward,J.J., Dreifus,J.E. and Merrikh,H. (2017) Replication-transcription conflicts generate R-loops that orchestrate bacterial stress survival and pathogenesis. *Cell*, **170**, 787–799.

28. Ge,X.Q., Jackson,D.A. and Blow,J.J. (2007) Dormant origins licensed by excess Mcm2-7 are required for human cells to survive replicative stress. *Genes Dev.*, **21**, 3331–3341.

29. Anglana,M., Apiou,F., Bensimon,A. and Debatisse,M. (2003) Dynamics of DNA replication in mammalian somatic cells: nucleotide pool modulates origin choice and interorigin spacing. *Cell*, **114**, 385–394.

30. Doksani,Y., Bermejo,R., Fiorani,S., Haber,J.E. and Foiani,M. (2009) Replicon dynamics, dormant origin firing, and terminal fork integrity after double-strand break formation. *Cell*, **137**, 247–258.

31. Ibarra,A., Schwob,E. and Mendez,J. (2008) Excess MCM proteins protect human cells from replicative stress by licensing backup origins of replication. *Proc. Natl. Acad. Sci. U.S.A.*, **105**, 8956–8961.

32. Madireddy,A., Kosiyatrakul,S.T., Boisvert,R.A., Herrera-Moyano,E., Garcia-Rubio,M.L., Gerhardt,J., Vuono,E.A., Owen,N., Yan,Z., Olson,S. *et al.* (2016) FANCD2 facilitates replication through common fragile sites. *Mol. Cell*, **64**, 388–404.

33. Santocanale,C. and Diffley,J.F. (1998) A Mec1- and Rad53-dependent checkpoint controls late-firing origins of DNA replication. *Nature*, **395**, 615–618.

34. Shirahige,K., Hori,Y., Shiraishi,K., Yamashita,M., Takahashi,K., Obuse,C., Tsurimoto,T. and Yoshikawa,H. (1998) Regulation of DNA-replication origins during cell-cycle progression. *Nature*, **395**, 618–621.

35. Yekezare,M., Gomez-Gonzalez,B. and Diffley,J.F. (2013) Controlling DNA replication origins in response to DNA damage—inhibit globally, activate locally. *J. Cell Sci.*, **126**, 1297–1306.

36. Storici,F. and Resnick,M.A. (2006) The delitto perfetto approach to in vivo site-directed mutagenesis and chromosome rearrangements with synthetic oligonucleotides in yeast. *Methods Enzymol.*, **409**, 329–345.

37. Liberi,G., Cotta-Ramusino,C., Lopes,M., Sogo,J., Conti,C., Bensimon,A. and Foiani,M. (2006) Methods to study replication fork collapse in budding yeast. *Methods Enzymol.*, **409**, 442–462.

38. Newman,T.J., Mamun,M.A., Nieduszynski,C.A. and Blow,J.J. (2013) Replisome stall events have shaped the distribution of replication origins in the genomes of yeasts. *Nucleic Acids Res.*, **41**, 9705–9718.

39. Brewer,B.J. and Fangman,W.L. (1988) A replication fork barrier at the 3′ end of yeast ribosomal RNA genes. *Cell*, **55**, 637–643.

40. Jossen,R. and Bermejo,R. (2013) The DNA damage checkpoint response to replication stress: a game of forks. *Front. Genet.*, **4**, 26.

41. Crabbe,L., Thomas,A., Pantesco,V., De Vos,J., Pasero,P. and Lengronne,A. (2010) Analysis of replication profiles reveals key role of RFC-Ctf18 in yeast replication stress response. *Nat. Struct. Mol. Biol.*, **17**, 1391–1397.

42. Osborn,A.J. and Elledge,S.J. (2003) Mrc1 is a replication fork component whose phosphorylation in response to DNA replication stress activates Rad53. *Genes Dev.*, **17**, 1755–1767.

43. Tittel-Elmer,M., Alabert,C., Pasero,P. and Cobb,J.A. (2009) The MRX complex stabilizes the replisome independently of the S phase checkpoint during replication stress. *EMBO J.*, **28**, 1142–1156.

44. Aze,A., Zhou,J.C., Costa,A. and Costanzo,V. (2013) DNA replication and homologous recombination factors: acting together to maintain genome stability. *Chromosoma*, **122**, 401–413.

45. Moreau,S., Ferguson,J.R. and Symington,L.S. (1999) The nuclease activity of Mre11 is required for meiosis but not for mating type switching, end joining, or telomere maintenance. *Mol. Cell. Biol.*, **19**, 556–566.

46. Duch,A., Felipe-Abrio,I., Barroso,S., Yaakov,G., Garcia-Rubio,M., Aguilera,A., de Nadal,E. and Posas,F. (2013) Coordinated control of replication and transcription by a SAPK protects genomic integrity. *Nature*, **493**, 116–119.

47. Kawabata,T., Luebben,S.W., Yamaguchi,S., Ilves,I., Matise,I., Buske,T., Botchan,M.R. and Shima,N. (2011) Stalled fork rescue via dormant replication origins in unchallenged S phase promotes proper chromosome segregation and tumor suppression. *Mol. Cell*, **41**, 543–553.

48. Blow,J.J. and Ge,X.Q. (2009) A model for DNA replication showing how dormant origins safeguard against replication fork failure. *EMBO Rep.*, **10**, 406–412.

49. Falaschi,A. (2000) Eukaryotic DNA replication: a model for a fixed double replisome. *Trends Genet.*, **16**, 88–92.

50. Dingman,C.W. (1974) Bidirectional chromosome replication: some topological considerations. *J. Theor. Biol.*, **43**, 187–195.

51. Kitamura,E., Blow,J.J. and Tanaka,T.U. (2006) Live-cell imaging reveals replication of individual replicons in eukaryotic replication factories. *Cell*, **125**, 1297–1308.

52. Lemon,K.P. and Grossman,A.D. (1998) Localization of bacterial DNA polymerase: evidence for a factory model of replication. *Science*, **282**, 1516–1519.

53. Wessel,R., Schweizer,J. and Stahl,H. (1992) Simian virus 40 T-antigen DNA helicase is a hexamer which forms a binary complex during bidirectional unwinding from the viral origin of DNA replication. *J. Virol.*, **66**, 804–815.

54. Reyes-Lamothe,R., Possoz,C., Danilova,O. and Sherratt,D.J. (2008) Independent positioning and action of Escherichia coli replisomes in live cells. *Cell*, **133**, 90–102.

55. Yardimci,H., Loveland,A.B., Habuchi,S., van Oijen,A.M. and Walter,J.C. (2010) Uncoupling of sister replisomes during eukaryotic DNA replication. *Mol. Cell*, **40**, 834–840.

56. Cotta-Ramusino,C., Fachinetti,D., Lucca,C., Doksani,Y., Lopes,M., Sogo,J. and Foiani,M. (2005) Exo1 processes stalled replication forks and counteracts fork reversal in checkpoint-defective cells. *Mol. Cell*, **17**, 153–159.

57. Qiu,J., Qian,Y., Chen,V., Guan,M.X. and Shen,B. (1999) Human exonuclease 1 functionally complements its yeast homologues in DNA recombination, RNA primer removal, and mutation avoidance. *J. Biol. Chem.*, **274**, 17893–17900.

58. Bentsen,I.B., Nielsen,I., Lisby,M., Nielsen,H.B., Gupta,S.S., Mundbjerg,K., Andersen,A.H. and Bjergbaek,L. (2013) MRX protects fork integrity at protein-DNA barriers, and its absence causes checkpoint activation dependent on chromatin context. *Nucleic Acids Res.*, **41**, 3173–3189.

59. Seeber,A., Hegnauer,A.M., Hustedt,N., Deshpande,I., Poli,J., Eglinger,J., Pasero,P., Gut,H., Shinohara,M., Hopfner,K.P. *et al.* (2016) RPA mediates recruitment of MRX to forks and double-strand breaks to hold sister chromatids together. *Mol. Cell*, **64**, 951–966.

60. Ray Chaudhuri,A., Callen,E., Ding,X., Gogola,E., Duarte,A.A., Lee,J.E., Wong,N., Lafarga,V., Calvo,J.A., Panzarino,N.J. *et al.* (2016) Replication fork stability confers chemoresistance in BRCA-deficient cells. *Nature*, **535**, 382–387.

61. Stracker,T.H. and Petrini,J.H. (2011) The MRE11 complex: starting from the ends. *Nat. Rev. Mol. Cell Biol.*, **12**, 90–103.